Defining Pupil Knowledge Requirements for Roman Space Telescope Integrated Payload Assembly Testing

M.S. Thesis Defense

Kaitlyn Summey

Cornell University, Aerospace Engineering

August 30, 2022

Joint work with NASA Goddard Space Flight Center

Outline

The Nancy G. Roman Space Telescope (RST)

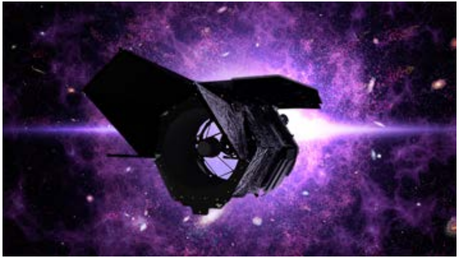

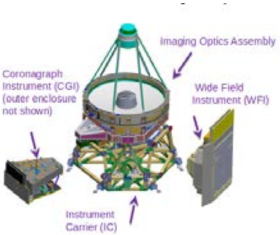

- NASA's next flagship observatory
- Will study multiple areas of astrophysics including universal expansion, dark energy, and exoplanets
- Two instruments on-board: the Wide-Field Instrument (WFI) and the Coronagraph Instrument (CGI) [a]

[a] NASA Goddard Space Flight Center. Roman space telescope mission overview. https://roman.gsfc.nasa.gov/about.html

Integrated Payload Testing

Test configuration in Space Environment Simulator

- Alignment verification of payload (WFI and imaging optics assembly)
- Will use internal and external optical components to understand how light travels through the telescope
- Conducted in Space Environment Simulator (SES) chamber at NASA Goddard[a]

[a] Bolcar et al., "Roman Space Telescope Optical System: Overview, Test, and Verification".

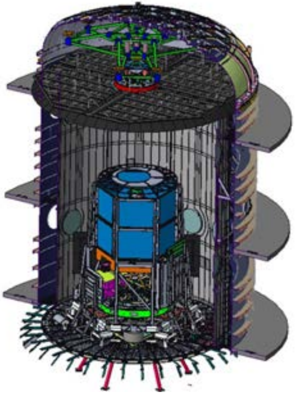

Figure: RST and ground support equipment in SES

Integrated Payload Testing

Test configuration in Space Environment Simulator

- Alignment verification of payload (WFI and imaging optics assembly)
- Will use internal and external optical components to understand how light travels through the telescope
- Conducted in Space Environment Simulator (SES) chamber at NASA Goddard[a]

[a] Bolcar et al., “Roman Space Telescope Optical System: Overview, Test, and Verification”.

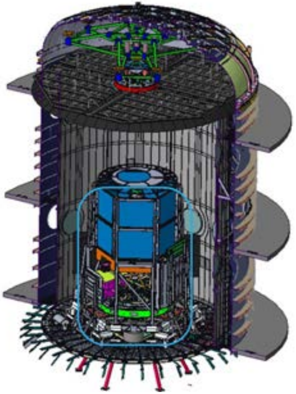

Figure: RST and ground support equipment in SES

Integrated Payload Testing

Test configuration in Space Environment Simulator

- Alignment verification of payload (WFI and imaging optics assembly)
- Will use internal and external optical components to understand how light travels through the telescope
- Conducted in Space Environment Simulator (SES) chamber at NASA Goddard[a]

[a] Bolcar et al., "Roman Space Telescope Optical System: Overview, Test, and Verification".

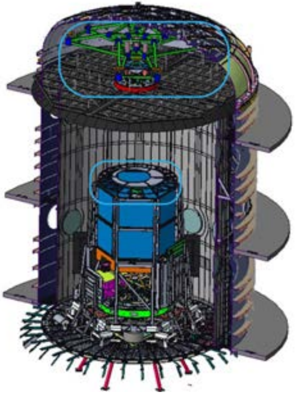

Figure: RST and ground support equipment in SES

Integrated Payload Testing

Telescope model not to scale

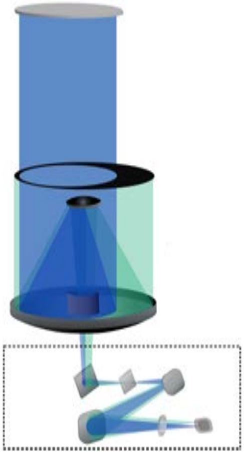

Figure: Wide-Field Instrument (WFI)

Integrated Payload Testing

Telescope model not to scale

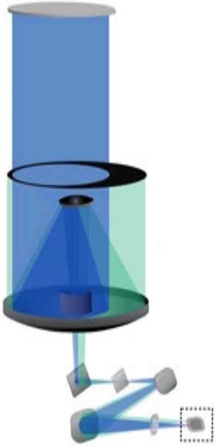

Figure: Focal Plane Array (FPA)

Integrated Payload Testing
Detector and sources

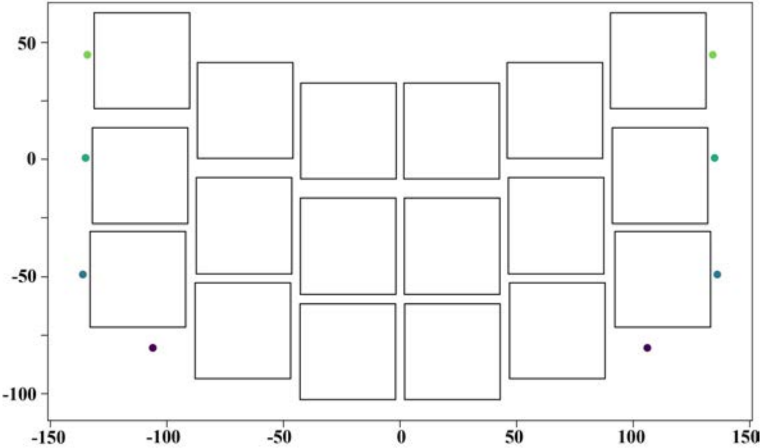

Figure: FPA detector configuration in mm

Integrated Payload Testing

Telescope model not to scale

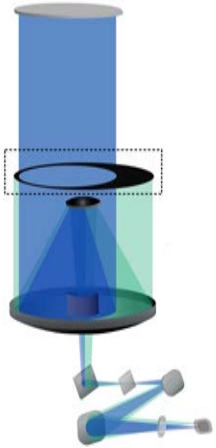

Figure: Subaperture Metrology System (SAMS)

Integrated Payload Testing

Telescope model not to scale

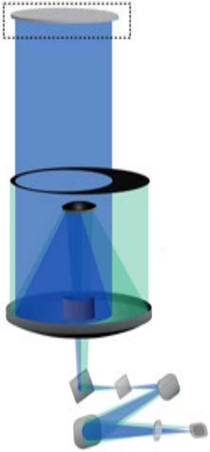

Figure: Optical Large Aperture Flat System (OLAFS)


WFI

Integrated Payload Testing

Pseudo double pass beam path

Integrated Payload Testing

Pseudo double pass beam path

Integrated Payload Testing
Pseudo double pass beam path

Integrated Payload Testing
Pseudo double pass beam path

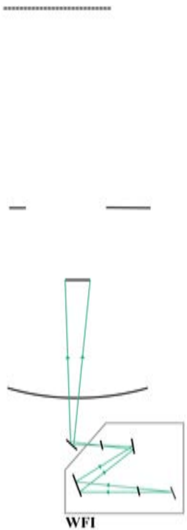

Integrated Payload Testing
Pseudo double pass beam path

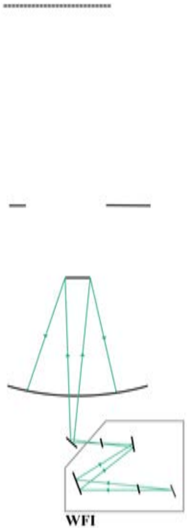

Integrated Payload Testing
Pseudo double pass beam path

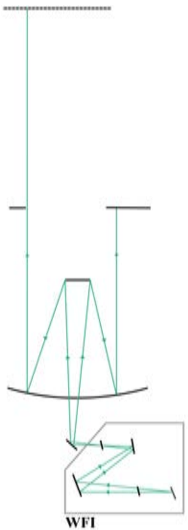

Integrated Payload Testing
Pseudo double pass beam path

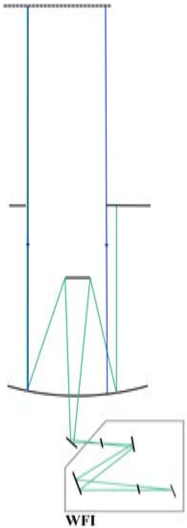

Integrated Payload Testing
Pseudo double pass beam path

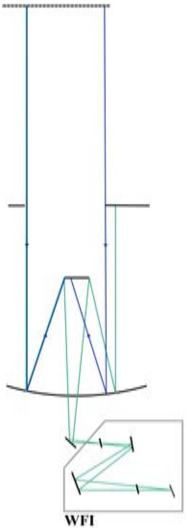

Integrated Payload Testing

Pseudo double pass beam path

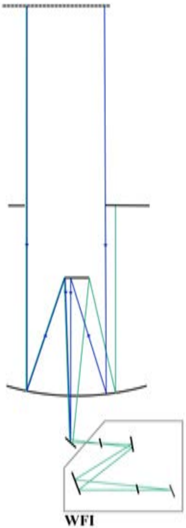

Integrated Payload Testing
Pseudo double pass beam path

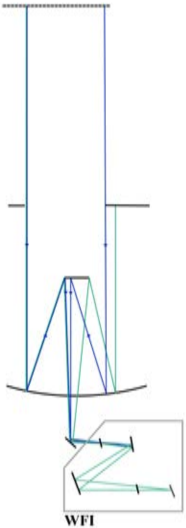

Integrated Payload Testing

Pseudo double pass beam path

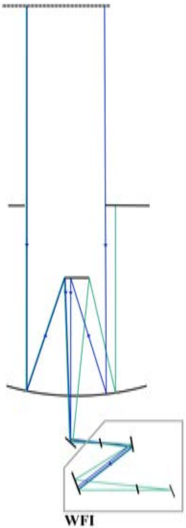

Integrated Payload Testing

Pseudo double pass beam path

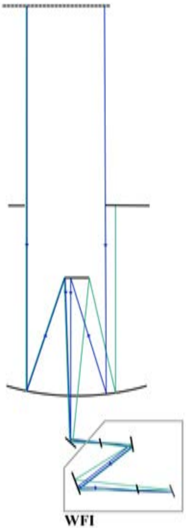

Integrated Payload Testing
Active components

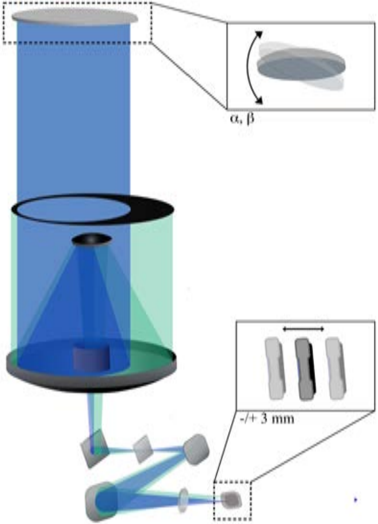

Integrated Payload Testing

Verify telescope alignment using image-based wavefront sensing

- Translate FPA through focus
- Illuminate fiber sources
- Tilt OLAFS to translate beams across the FPA and sample entire field of view[a]
- Image point sources on the detector
- Reconstruct wavefront based on system knowledge and image of point source

[a] Bergkoetter and Jurling, “Data analysis algorithm for double-pass testing of the Roman Space Telescope”.

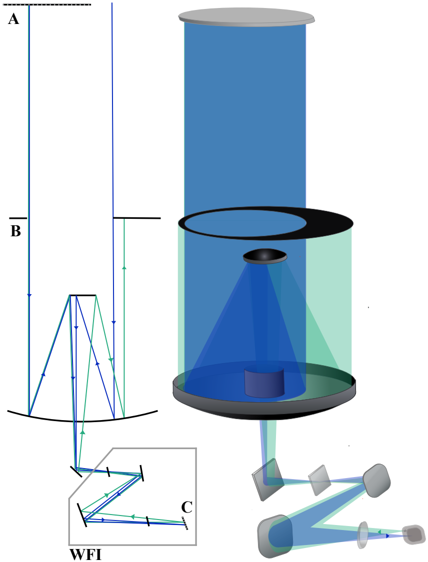

Integrated Payload Testing

Verify telescope alignment using image-based wavefront sensing

- Phase retrieval will be used throughout RST integration
- Will not be able to offload gravity on the primary mirror after integrating payload
- Most realistic option for wavefront sensing that can accommodate gravity induced aberrations

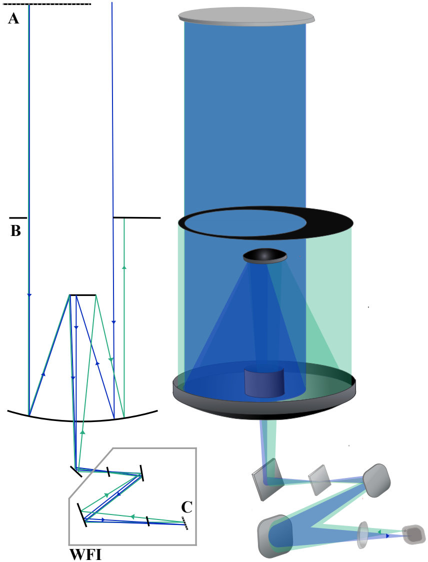

Integrated Payload Testing

Point sources on detector through test pass for 6 OLAFS tilts

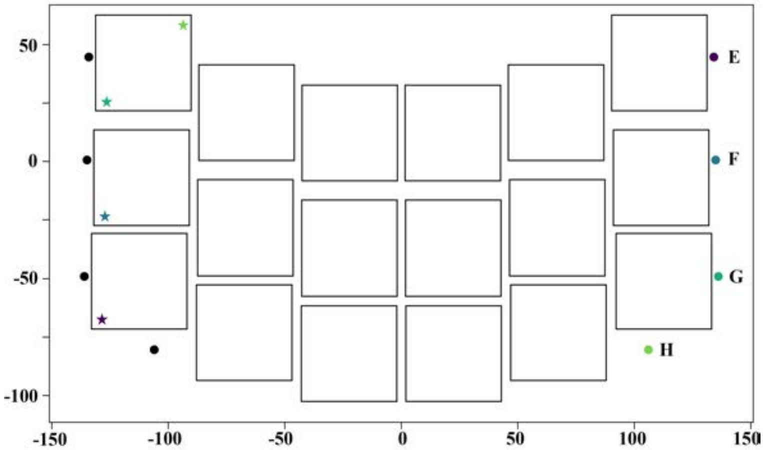

Figure: FPA detector configuration in mm

Integrated Payload Testing

Point sources on detector through test pass for 6 OLAFS tilts

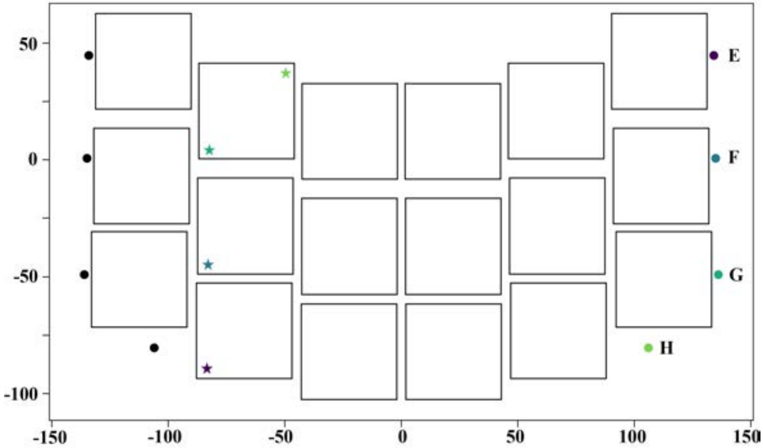

Figure: FPA detector configuration in mm

Integrated Payload Testing

Point sources on detector through test pass for 6 OLAFS tilts

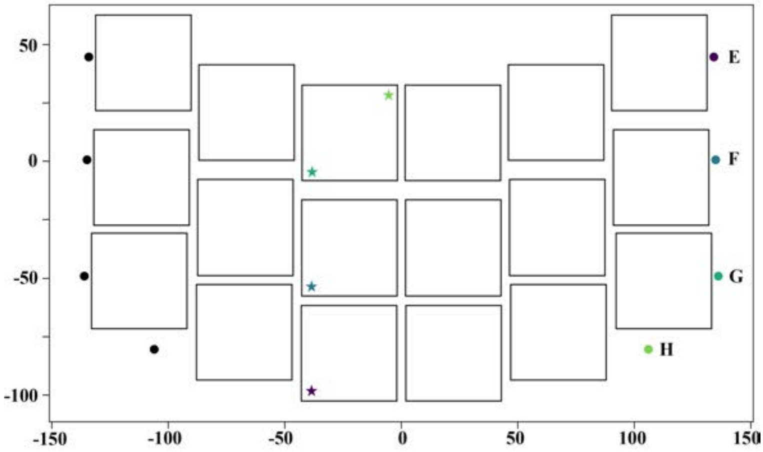

Figure: FPA detector configuration in mm

Integrated Payload Testing

Point sources on detector through test pass for 6 OLAFS tilts

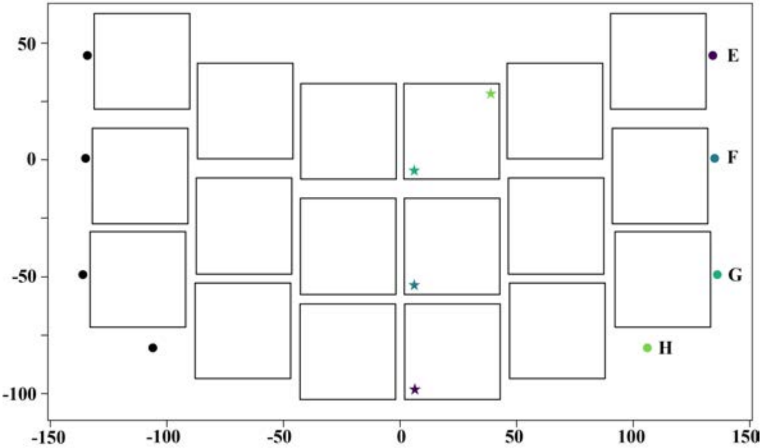

Figure: FPA detector configuration in mm

Integrated Payload Testing

Point sources on detector through test pass for 6 OLAFS tilts

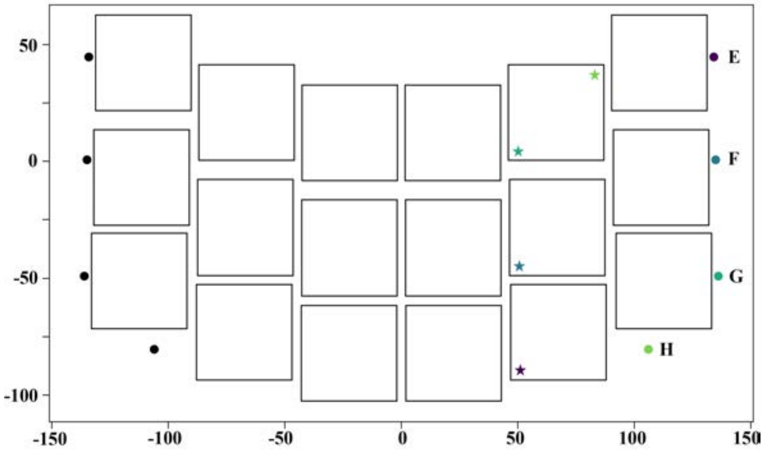

Figure: FPA detector configuration in mm

Integrated Payload Testing

Point sources on detector through test pass for 6 OLAFS tilts

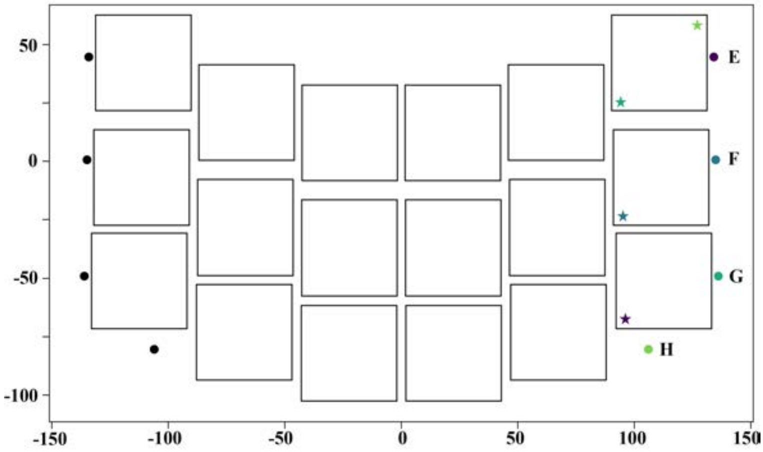

Figure: FPA detector configuration in mm

Fourier Optics Review

- Background
- Diffraction
- Field propagation

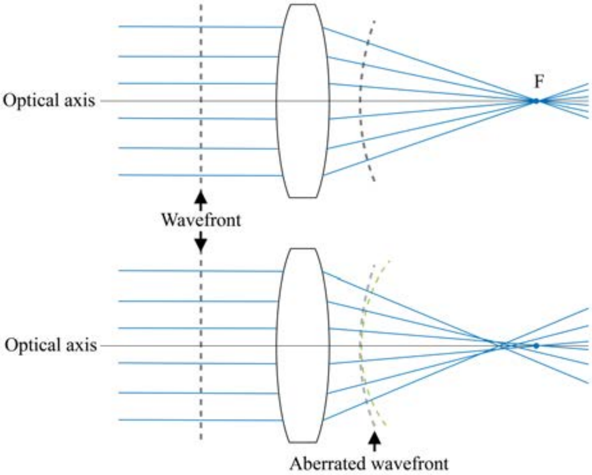

F
Optical axis
Wavefront
Optical axis
Aberrated wavefront

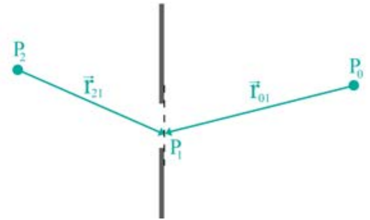

$$U(P_1) = \frac{Ae^{jkr_{21}}}{r_{21}}$$

$U(P_1)$ aperture illumination from single spherical wave diverging from a point source P_2[a]

[a]Goodman, *Introduction to Fourier Optics*.

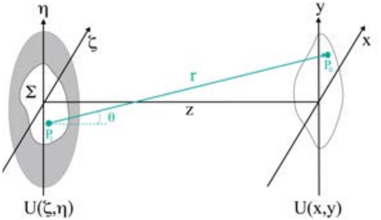

$$U(P_0) = \frac{1}{j\lambda}\iint_{\Sigma} U(P_1)\frac{e^{jkr}}{r}\cos\theta ds$$

$U(P_0)$ complex field disturbance at P_0

λ wavelength

k wave number

Σ enclosed space around P_1 [a]

[a] Goodman, *Introduction to Fourier Optics*.

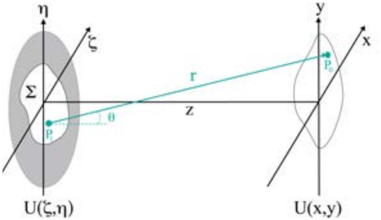

$$\cos\theta = \frac{z}{r}$$

Rewrite as[a]

$$U(x,y) = \frac{1}{j\lambda z} \iint_{\Sigma} U(\xi,\eta) \frac{e^{jkr}}{r^2} ds$$

[a] Goodman, *Introduction to Fourier Optics*.

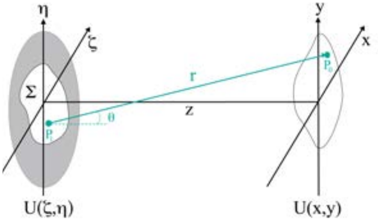

$$U(x,y) = \iint_{-\infty}^{\infty} U(\xi,\eta)\frac{e^{jkr}}{r^2}d\xi d\eta$$

$$r = \sqrt{z^2 + (x-\xi)^2 + (y-\eta)^2}$$

$$r \cong z + \frac{(x-\xi)^2 + (y-\eta)^2}{2z}$$

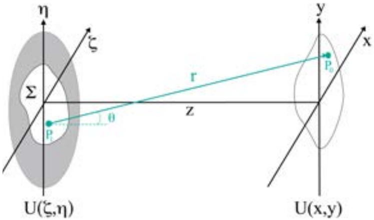

Plugging in the approximation for r, we get the Fresnel diffraction integral[a]

$$U(x,y) = \frac{e^{jkz}}{j\lambda z} e^{\frac{jk}{2z}(x^2+y^2)} \iint_{-\infty}^{\infty} U(\xi,\eta) e^{\frac{jk}{2z}(\xi^2+\eta^2)} e^{\frac{-j2\pi}{\lambda z}(x\xi+y\eta)} d\xi d\eta$$

[a] Goodman, *Introduction to Fourier Optics*.

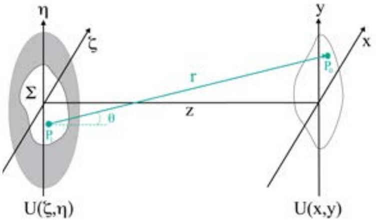

Plugging in the approximation for r, we get the Fresnel diffraction integral[a]

$$U(x,y) = \frac{e^{jkz}}{j\lambda z} e^{\frac{jk}{2z}(x^2+y^2)} \iint_{-\infty}^{\infty} U(\xi,\eta) e^{\frac{jk}{2z}(\xi^2+\eta^2)} e^{\frac{-j2\pi}{\lambda z}(x\xi+y\eta)} d\xi d\eta$$

[a] Goodman, *Introduction to Fourier Optics*.

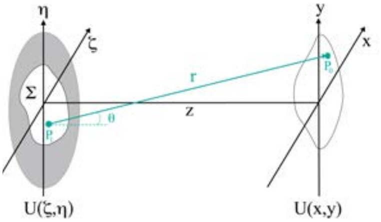

Plugging in the approximation for r, we get the Fresnel diffraction integral[a]

$$U(x,y) = \frac{e^{jkz}}{j\lambda z} e^{\frac{jk}{2z}(x^2+y^2)} \iint_{-\infty}^{\infty} U(\xi,\eta) e^{\frac{jk}{2z}(\xi^2+\eta^2)} e^{\frac{-j2\pi}{\lambda z}(x\xi+y\eta)} d\xi d\eta$$

[a] Goodman, *Introduction to Fourier Optics*.

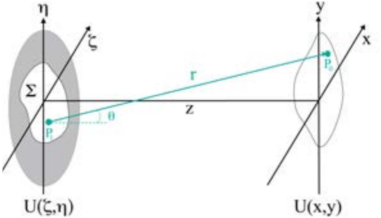

Plugging in the approximation for r, we get the Fresnel diffraction integral[a]

$$U(x,y) = \frac{e^{jkz}}{j\lambda z} e^{\frac{jk}{2z}(x^2+y^2)} \iint_{-\infty}^{\infty} U(\xi,\eta) e^{\frac{jk}{2z}(\xi^2+\eta^2)} e^{\frac{-j2\pi}{\lambda z}(x\xi+y\eta)} d\xi d\eta$$

[a] Goodman, *Introduction to Fourier Optics*.

Phase Retrieval

- Phase retrieval and space telescopes
- Application of field propagation
- Algorithm background
  - Iterative approach
  - Nonlinear optimization
  - Algorithmic differentiation

Phase Retrieval
Brief history

Phase retrieval was used to characterize Hubble mirror flaw[a]

James Webb Space Telescope demonstrated that phase retrieval is a useful and necessary method of wavefront sensing that can be used through the stages of integration to on-sky alignment[b,c,d]

- Used for verification in ground testing
- Sole method of wavefront sensing for on-sky alignment

[a] Fienup, "Phase-retrieval algorithms for a complicated optical system".

[b] Smith et al., "Methodology and Results of James Webb Space Telescope Thermal Vacuum Optical System Alignment Testing and Analysis".

[c] Dean et al., "Phase retrieval algorithm for JWST Flight and Testbed Telescope".

[d] Aronstein et al., "Wavefront-error performance characterization for the James Webb Space Telescope (JWST) Integrated Science Instrument Module (ISIM) science instruments".

Figure: Pupil function

Wavefront error is defined as

$$\mathbf{W} = \sum_n a_n \mathbf{Z}_n,$$

where a_n are coefficients of a basis $\mathbf{Z}_n$ Using $\mathbf{W}$ we define the pupil function $\mathbf{g}$

$$\mathbf{g} = \mathbf{A} \circ e^{\left(\frac{i2\pi}{\lambda}\mathbf{W}\right)}$$

with $\mathbf{A}$ being the amplitude function and $\circ$ being element-wise multiplication[a]

[a] Fienup, "Phase retrieval algorithms: a comparison".

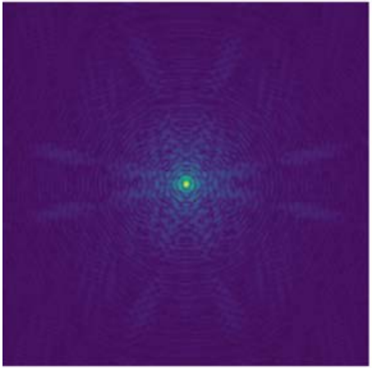

Figure: Modeled point spread function

We propagate from the pupil plane to the image plane $\mathbf{G}$ with a Fourier transform

$$\mathbf{G} = \mathcal{DFT}\{\mathbf{g}\}$$

The intensity I is the modeled point spread function for the forward model[a][b]

$$\mathbf{I} = |\mathbf{G}|^2$$

[a] Fienup, "Phase retrieval algorithms: a comparison".

[b] Fienup, "Phase-retrieval algorithms for a complicated optical system".

Phase Retrieval
Iterative algorithm (Gerberg-Saxton)

- Starts with wavefront guess and performs field propagation while adjusting parameters until the model sufficiently matches the measured data[a]
- Can be straightforward to implement- few lines of code
- Difficult to scale algorithm for complicated problems
- Can be prone to stagnation

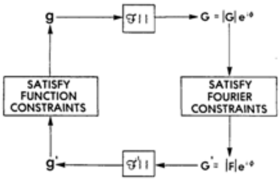

Figure: Gergberg-Saxton algorithm [1]

[a] Gerchberg, "A practical algorithm for the determination of phase from image and diffraction plane pictures".

[1] Fienup, "Phase retrieval algorithms: a comparison".

Phase Retrieval

Nonlinear optimization approach

The error metric ϵ is the sum of squares difference between our modeled point spread function and the measured data D

$$\epsilon = \frac{\sum_m w \circ (\alpha \mathbf{I}_m + \beta - \mathbf{D}_m)^2}{\sum_n^N w_n \circ \mathbf{D}_n^2}$$

where w is a weighing function to account for noise and bad pixels in the measured data

α and β are model parameters to account for gain and bias in the measured data

- Error metric is minimized using nonlinear optimization
- Gradients are constructed using algorithmic differentiation[a][b]

[a] Jurling and Fienup, "Applications of algorithmic differentiation to phase retrieval algorithms".

[b] Fienup, "Phase retrieval algorithms: a comparison".

Phase Retrieval

Algorithmic differentiation

$$\mathbf{W} = \sum_n a_n \mathbf{Z}_n,$$

$$\mathbf{g} = \mathbf{A} \circ e^{\left(\frac{i2\pi}{\lambda}\mathbf{W}\right)}$$

$$\mathbf{G} = \mathcal{DFT}\{\mathbf{g}\}$$

$$\mathbf{I} = |\mathbf{G}|^2$$

$$\epsilon = \frac{\sum_m w_m \circ (\alpha \mathbf{I}_m + \beta - \mathbf{D}_m)^2}{\sum_n^N w_n \circ \mathbf{D}_n^2}.$$

$$\bar{a_n} = \sum_p (\bar{\mathbf{W}}_p \mathbf{Z}_{n,p})$$

$$\bar{\mathbf{W}} = \frac{2\pi}{\lambda} \Im[\bar{\mathbf{g}} \circ \mathbf{g}^*]$$

$$\bar{\mathbf{g}} = \mathcal{IDFT}\{\bar{\mathbf{G}}\}$$

$$\bar{\mathbf{G}} = 2\mathbf{G} \circ \bar{\mathbf{I}}$$

$$\bar{\mathbf{I}} = 2\alpha w \circ (\alpha \mathbf{I}_m + \beta - \mathbf{D}_m)$$

- Works through steps in forward model to propagate gradients
- Use gradients to search along parameters in direction that minimizes error metric[a]

[a] Jurling and Fienup, "Applications of algorithmic differentiation to phase retrieval algorithms".

Project Background

- Motivation for study
  - Challenges for IPA testing
- Wavefront sensing considerations
  - Geometry of pupil during IPA testing
  - Effects of ground support equipment misalignment

- Phase retrieval is generally dependent on a well understood system
- The ground support equipment (SAMS and OLAFS) position will effect this system understanding
- The extreme environmental changes within the chamber can lead to temperature deformation of the SAMS which introduces knowledge error in the phase retrieval

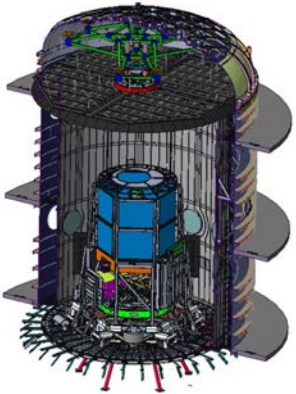

Figure: RST and ground support equipment in SES

Project Background

Effect of component decentering on pupil

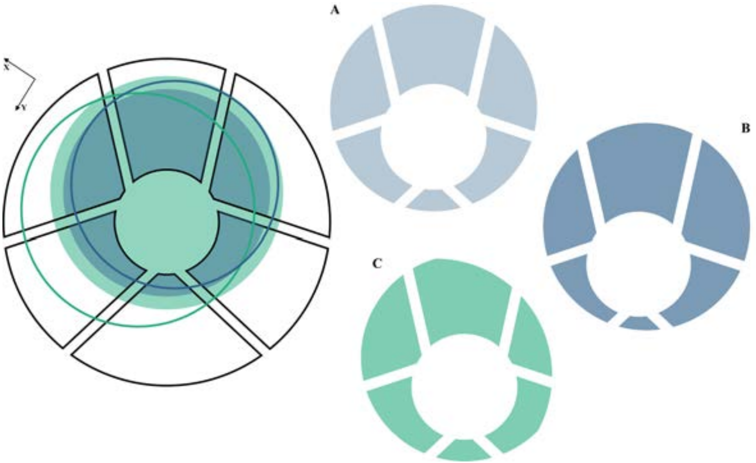

Project Background

Effect of component decentering on fitting

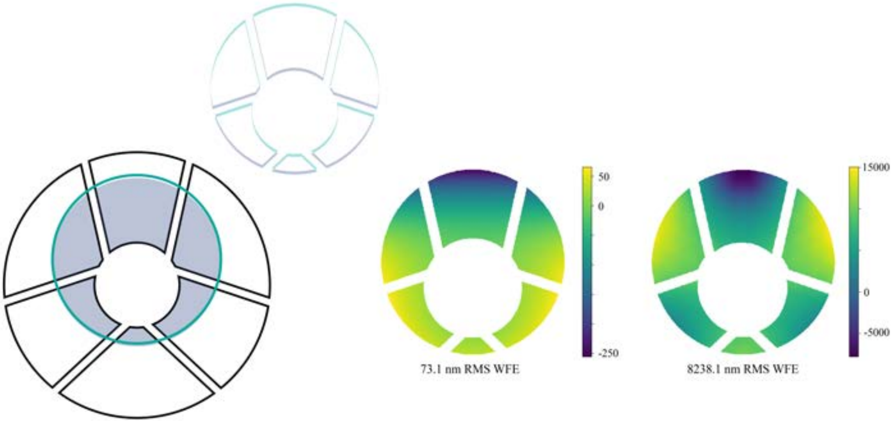

Project Background

Effect of component decentering on fitting

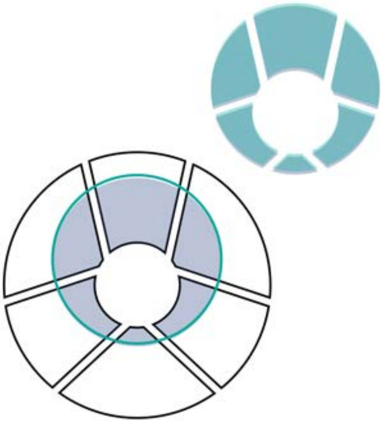

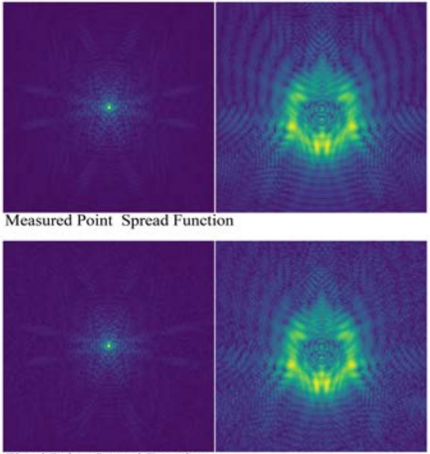

Measured Point Spread Function

Fitted Point Spread Function

Project Background

Pupil geometry of pseudo double pass

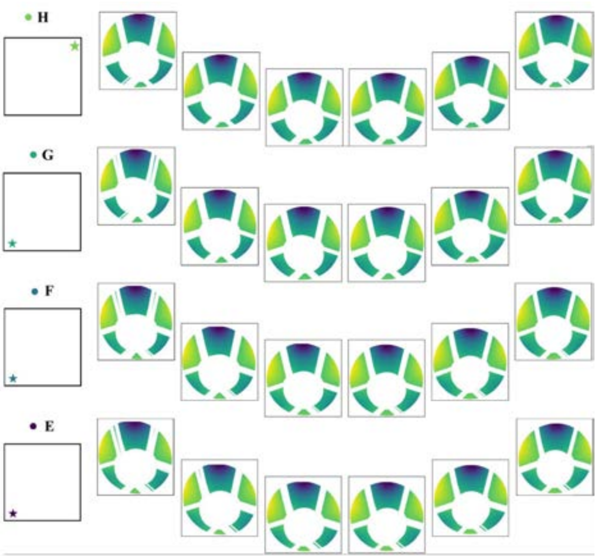

Project Background
Pupil geometry of pseudo double pass

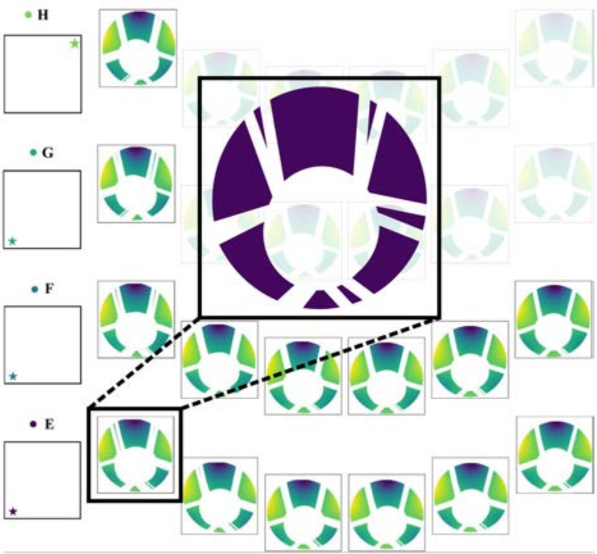

Project Background

Phase retrieval algorithm for study

- Goal is characterization not compensation
- Want to fully understand the effects of pupil knowledge error
- Optimized over tip/tilt, low-order Zernike functions, and a point-by-point fit[a]

[a] Jurling, Bergkoetter, and Fienup, “Techniques for arbitrary sampling in two-dimensional Fourier transforms”.

Overview of Models

Ideal model

- No surface aberrations or misalignment

Monte Carlo perturbed models

- 30 models generated with perturbed surfaces
- Simulates possible misalignment/surface errors
- No gravity sag

Gravity sag model

- Simulates aberration due to gravity sag on primary mirror

Monte Carlo study overview

Simulation

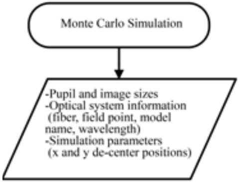

a b

[a] Jurling, "Advances in algorithms for image based wavefront sensing".

[b] Bergkoetter, "Phase retrieval for chromatic aberrations and wide-field detectors".

Simulation

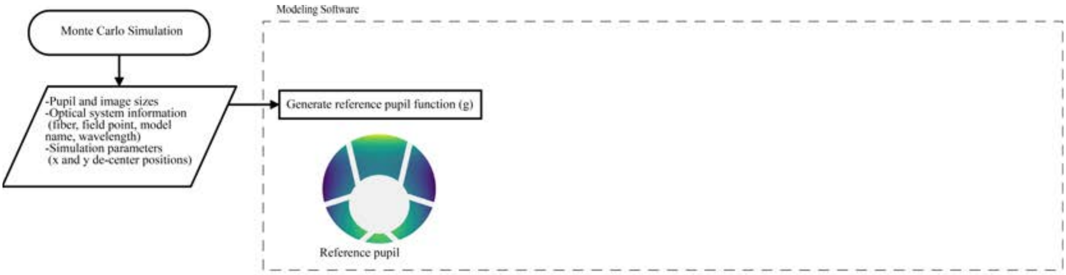

Modeling Software
Monte Carlo Simulation
-Pupil and image sizes
-Optical system information
(fiber, field point, model
name, wavelength)
-Simulation parameters
(x and y de-center positions)
Generate reference pupil function (g)
Reference pupil

Simulation

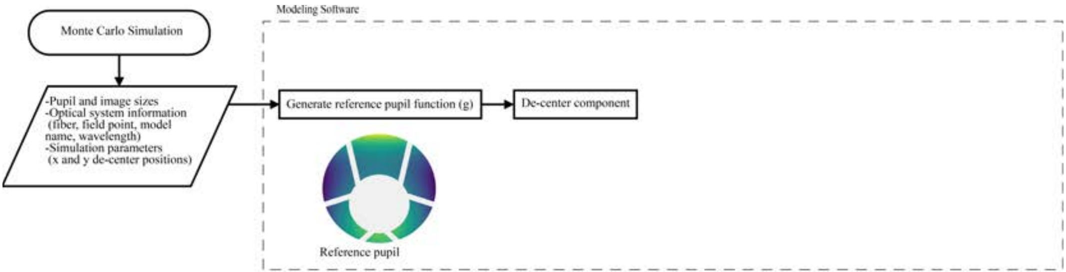

Monte Carlo Simulation
-Pupil and image sizes
-Optical system information
(fiber, field point, model
name, wavelength)
-Simulation parameters
(x and y de-center positions)
Modeling Software
Generate reference pupil function (g)
De-center component
Reference pupil

Simulation

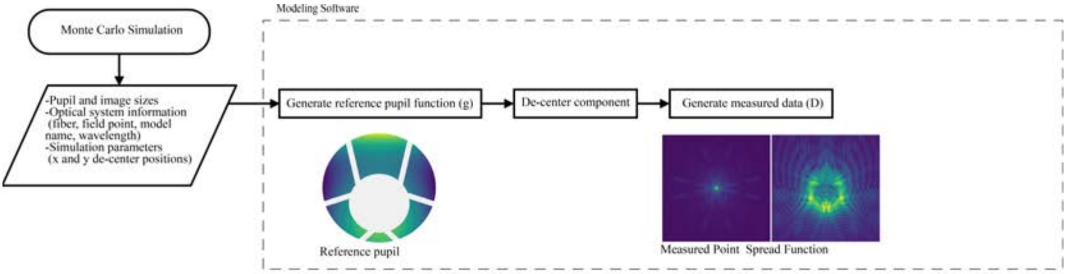

Modeling Software
Monte Carlo Simulation
-Pupil and image sizes
-Optical system information
(fiber, field point, model
name, wavelength)
-Simulation parameters
(x and y de-center positions)
Generate reference pupil function (g)
De-center component
Generate measured data (D)
Reference pupil
Measured Point Spread Function

Simulation

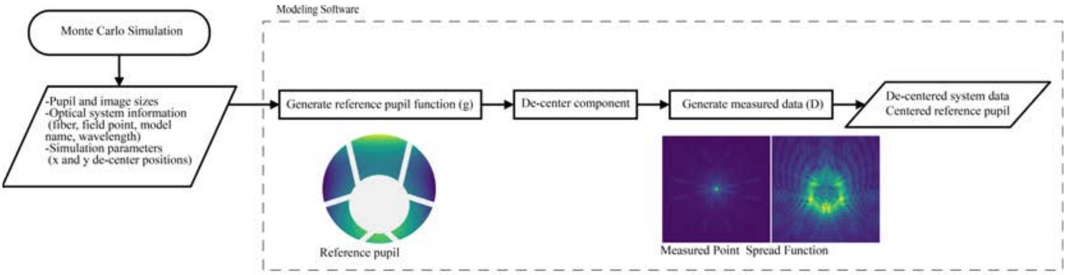

Modeling Software
Monte Carlo Simulation
-Pupil and image sizes
-Optical system information
(fiber, field point, model name, wavelength)
-Simulation parameters
(x and y de-center positions)
Generate reference pupil function (g)
De-center component
Generate measured data (D)
De-centered system data
Centered reference pupil
Reference pupil
Measured Point Spread Function

Simulation

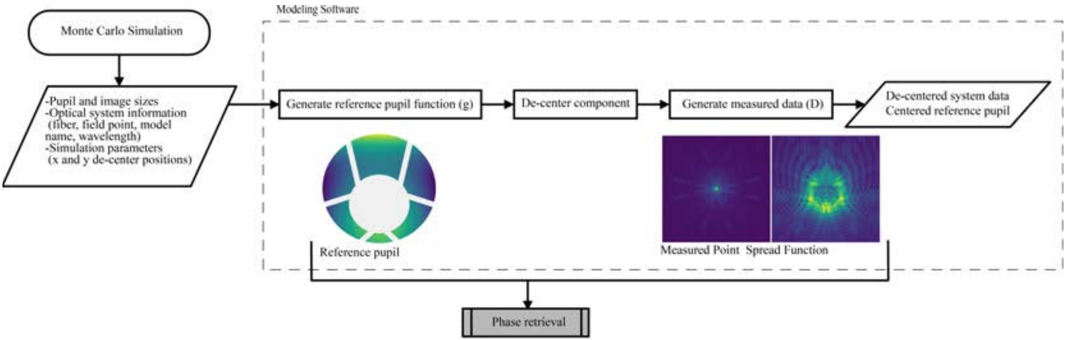
Modeling Software
Monte Carlo Simulation
-Pupil and image sizes
-Optical system information
(fiber, field point, model
name, wavelength)
-Simulation parameters
(x and y de-center positions)
Generate reference pupil function (g)
De-center component
Generate measured data (D)
De-centered system data
Centered reference pupil
Reference pupil
Measured Point Spread Function
Phase retrieval

Simulation

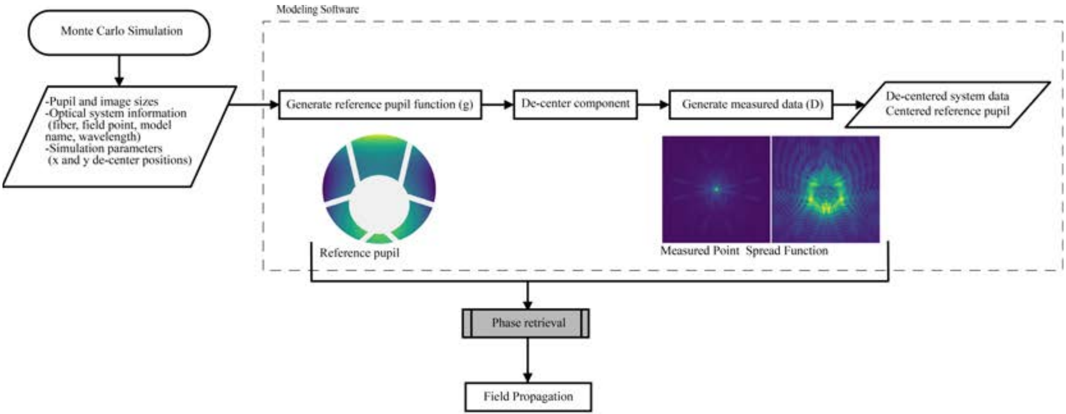
Modeling Software
Monte Carlo Simulation
-Pupil and image sizes
-Optical system information
(fiber, field point, model name, wavelength)
-Simulation parameters
(x and y de-center positions)
Generate reference pupil function (g)
De-center component
Generate measured data (D)
De-centered system data
Centered reference pupil
Reference pupil
Measured Point Spread Function
Phase retrieval
Field Propagation

Simulation

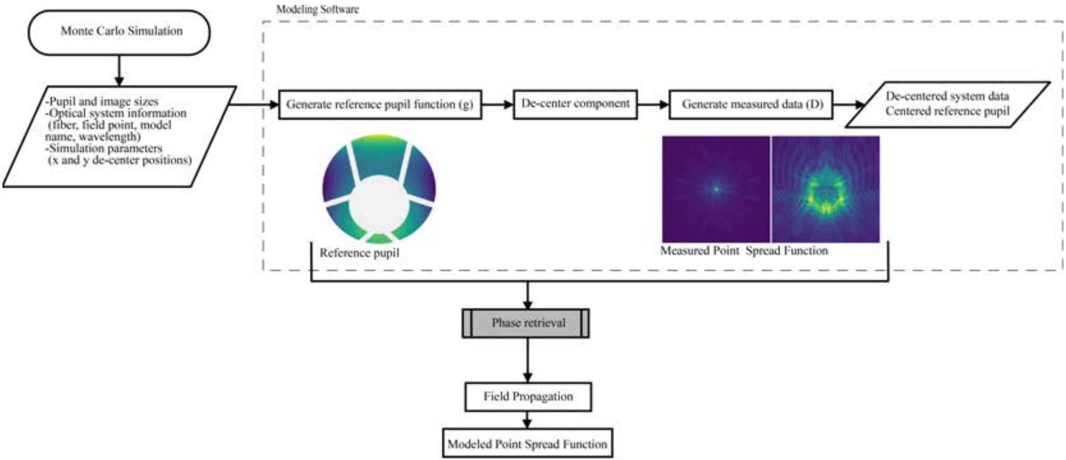

Monte Carlo Simulation
-Pupil and image sizes
-Optical system information (fiber, field point, model name, wavelength)
-Simulation parameters (x and y de-center positions)
Modeling Software
Generate reference pupil function (g)
De-center component
Generate measured data (D)
De-centered system data
Centered reference pupil
Reference pupil
Measured Point Spread Function
Phase retrieval
Field Propagation
Modeled Point Spread Function

Simulation

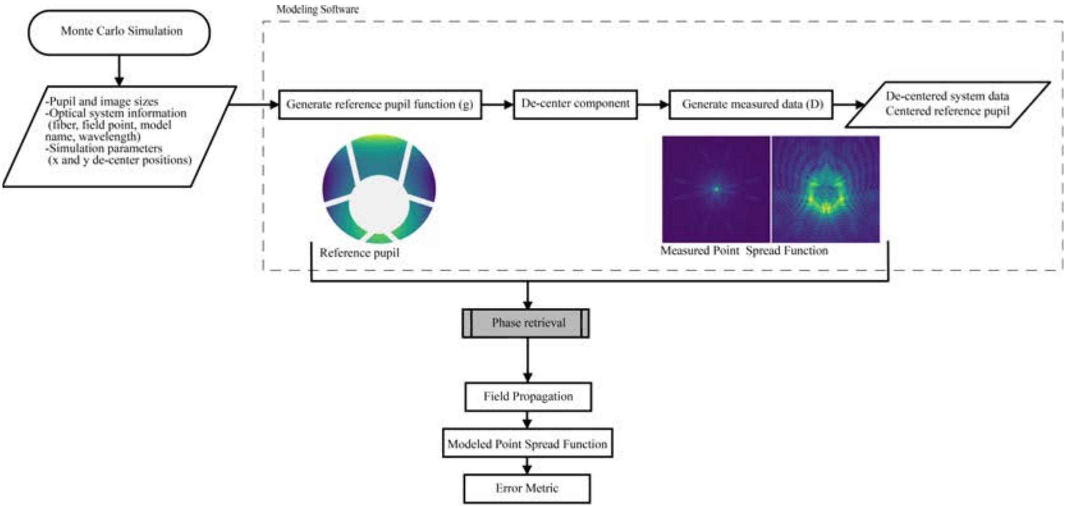

Modeling Software
Monte Carlo Simulation
-Pupil and image sizes
-Optical system information
(fiber, field point, model
name, wavelength)
-Simulation parameters
(x and y de-center positions)
Generate reference pupil function (g)
De-center component
Generate measured data (D)
De-centered system data
Centered reference pupil
Reference pupil
Measured Point Spread Function
Phase retrieval
Field Propagation
Modeled Point Spread Function
Error Metric

Simulation

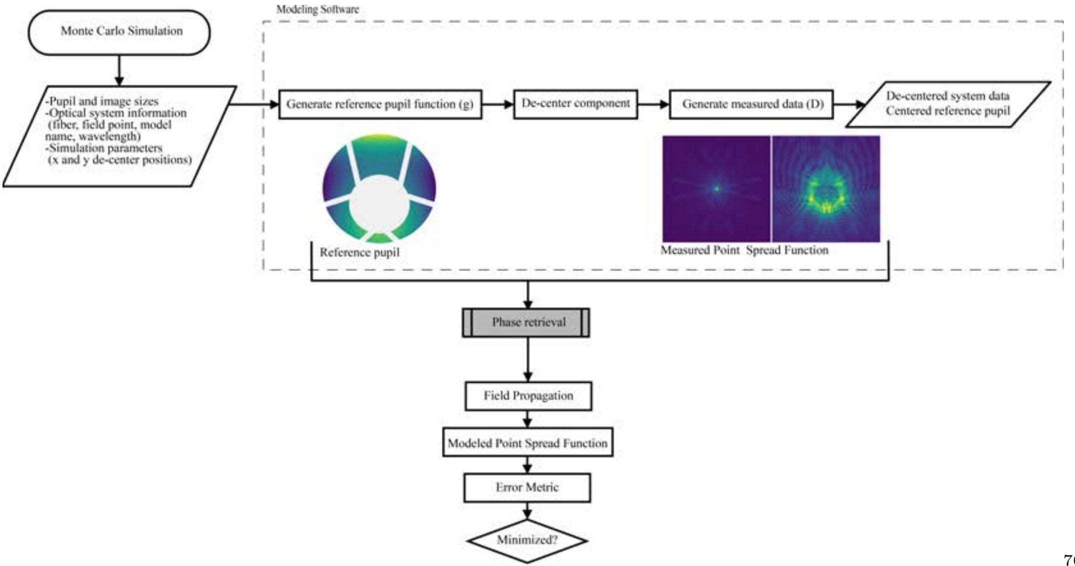

Modeling Software
Monte Carlo Simulation
-Pupil and image sizes
-Optical system information
(fiber, field point, model
name, wavelength)
-Simulation parameters
(x and y de-center positions)
Generate reference pupil function (g)
De-center component
Generate measured data (D)
De-centered system data
Centered reference pupil
Reference pupil
Measured Point Spread Function
Phase retrieval
Field Propagation
Modeled Point Spread Function
Error Metric
Minimized?

Simulation

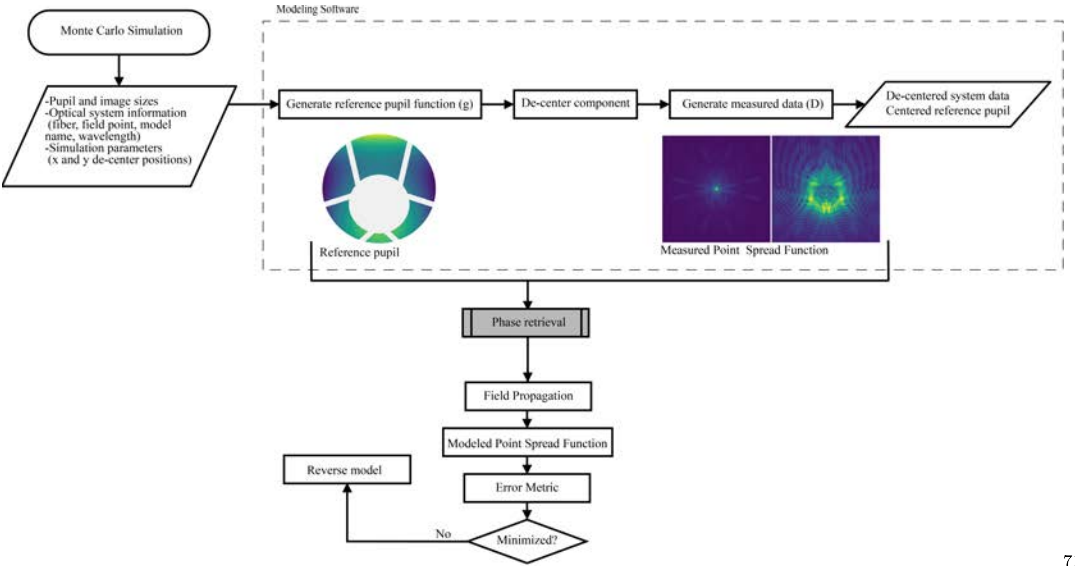

Modeling Software
Monte Carlo Simulation
-Pupil and image sizes
-Optical system information (fiber, field point, model name, wavelength)
-Simulation parameters (x and y de-center positions)
Generate reference pupil function (g)
De-center component
Generate measured data (D)
De-centered system data
Centered reference pupil
Reference pupil
Measured Point Spread Function
Phase retrieval
Field Propagation
Modeled Point Spread Function
Reverse model
Error Metric
No
Minimized?

Simulation

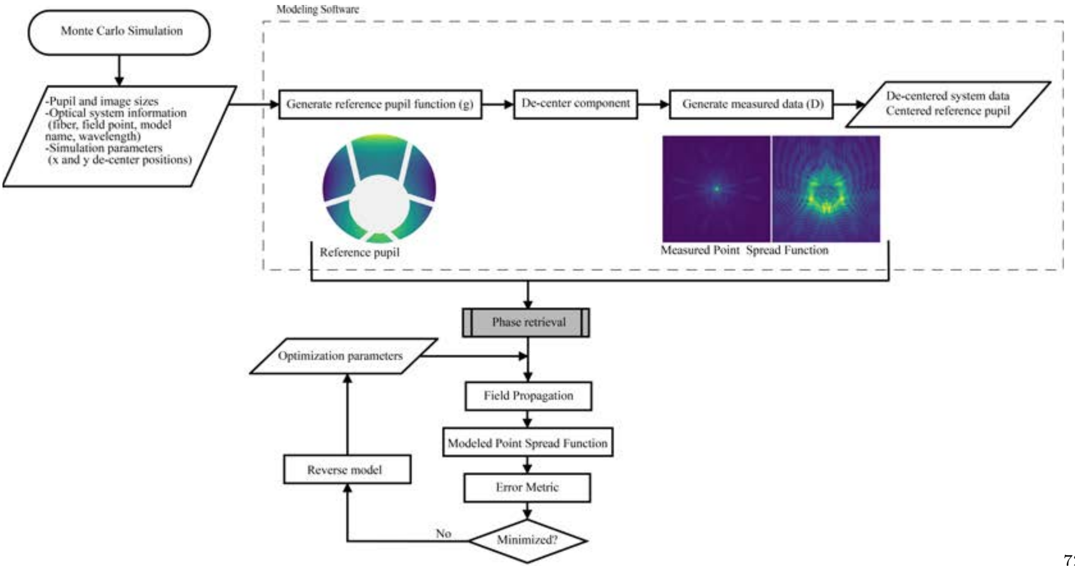

Modeling Software
Monte Carlo Simulation
-Pupil and image sizes
-Optical system information (fiber, field point, model name, wavelength)
-Simulation parameters (x and y de-center positions)
Generate reference pupil function (g)
De-center component
Generate measured data (D)
De-centered system data
Centered reference pupil
Reference pupil
Measured Point Spread Function
Phase retrieval
Optimization parameters
Field Propagation
Modeled Point Spread Function
Reverse model
Error Metric
No
Minimized?

Simulation

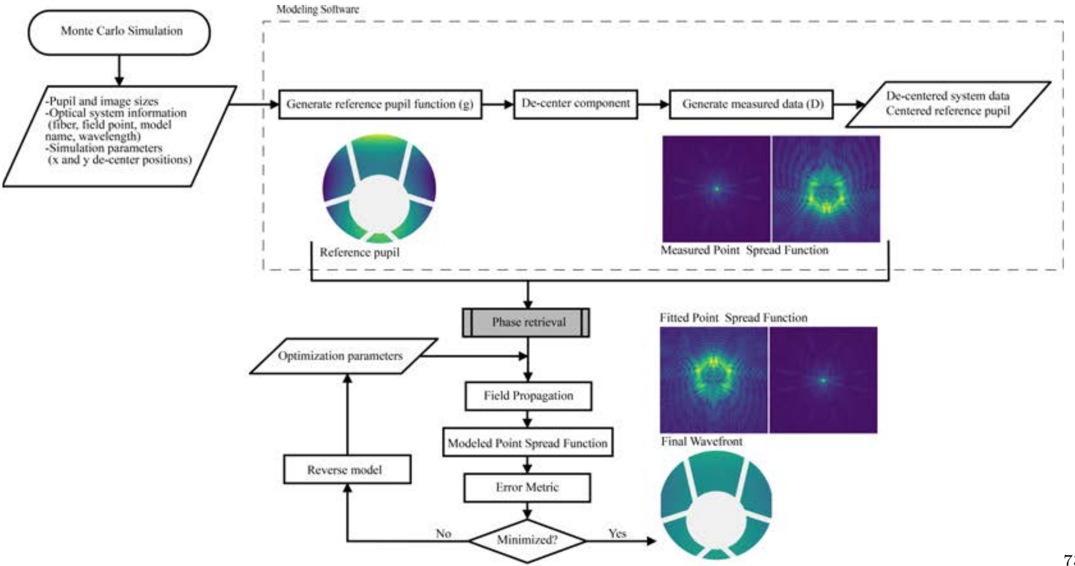

Modeling Software
Monte Carlo Simulation
-Pupil and image sizes
-Optical system information
(fiber, field point, model name, wavelength)
-Simulation parameters
(x and y de-center positions)
Generate reference pupil function (g)
De-center component
Generate measured data (D)
De-centered system data
Centered reference pupil
Reference pupil
Measured Point Spread Function
Phase retrieval
Optimization parameters
Field Propagation
Modeled Point Spread Function
Error Metric
Reverse model
Minimized?
No
Yes
Fitted Point Spread Function
Final Wavefront

Simulation

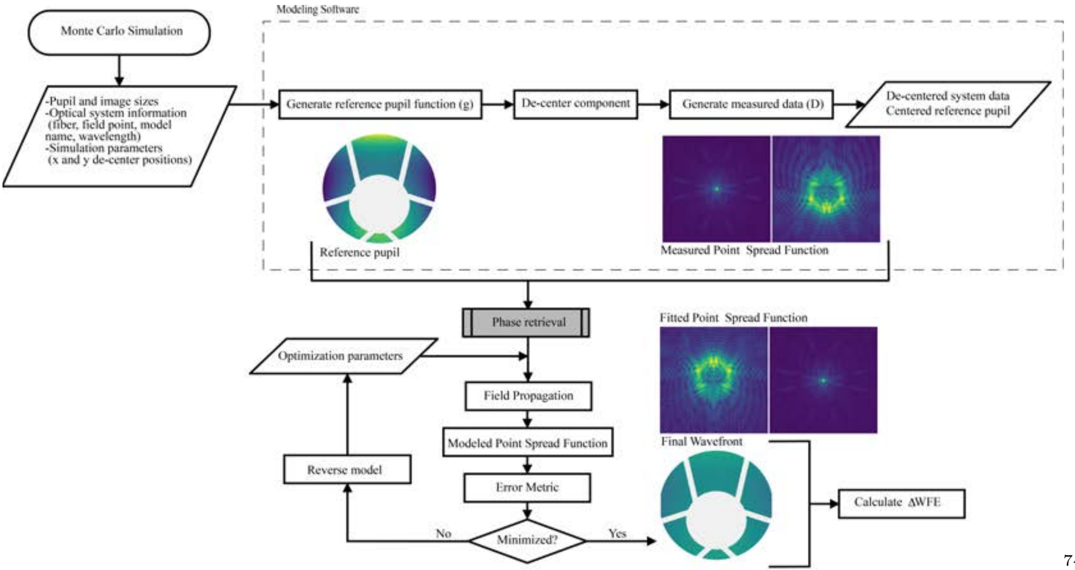
Monte Carlo Simulation
-Pupil and image sizes
-Optical system information
(fiber, field point, model name, wavelength)
-Simulation parameters
(x and y de-center positions)
Modeling Software
Generate reference pupil function (g)
De-center component
Generate measured data (D)
De-centered system data
Centered reference pupil
Reference pupil
Measured Point Spread Function
Phase retrieval
Optimization parameters
Field Propagation
Modeled Point Spread Function
Error Metric
Minimized?
No
Yes
Reverse model
Fitted Point Spread Function
Final Wavefront
Calculate ΔWFE

Results

Ideal model

- Contour plots
- Analysis across field of view
- Comparison of fiber locations

Perturbed models

- Box plot of results

Gravity sag model

- Contour plots
- Analysis across field of view
- Effects of model complications

Results
Ideal model baseline decentering study

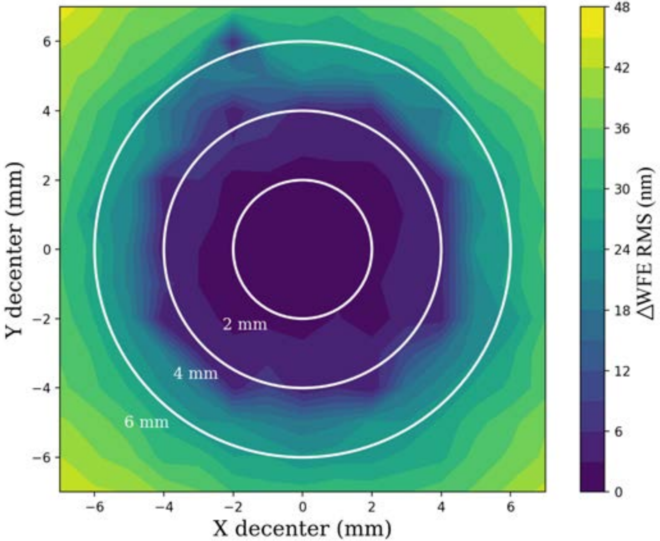

Results

Decentering contours across field of view

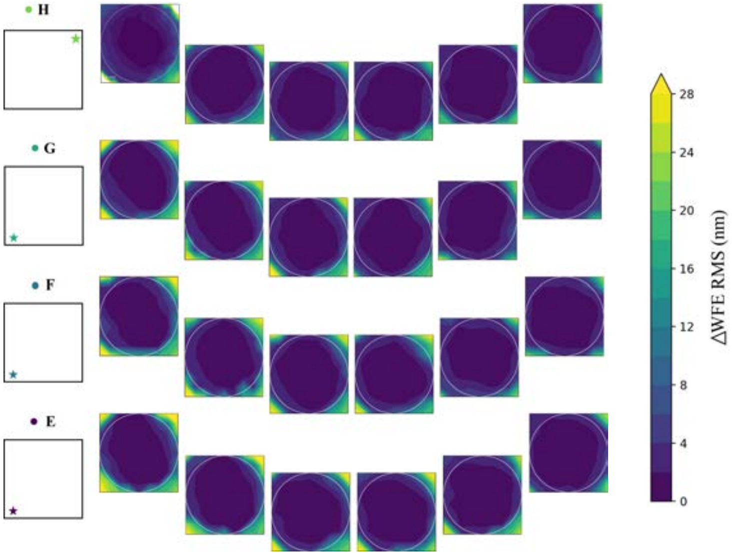

Results

95th percentile and max WFE within 4 mm decentering radius

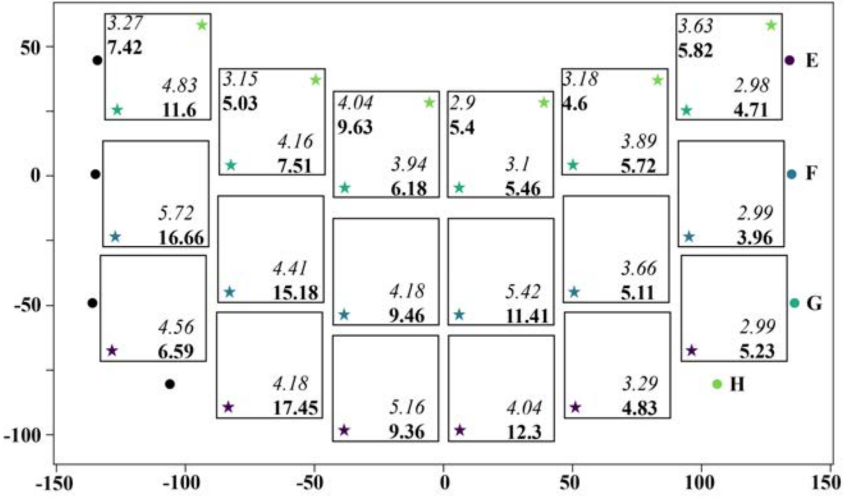

Results
Pupil geometry

Results

Pupil geometry effects

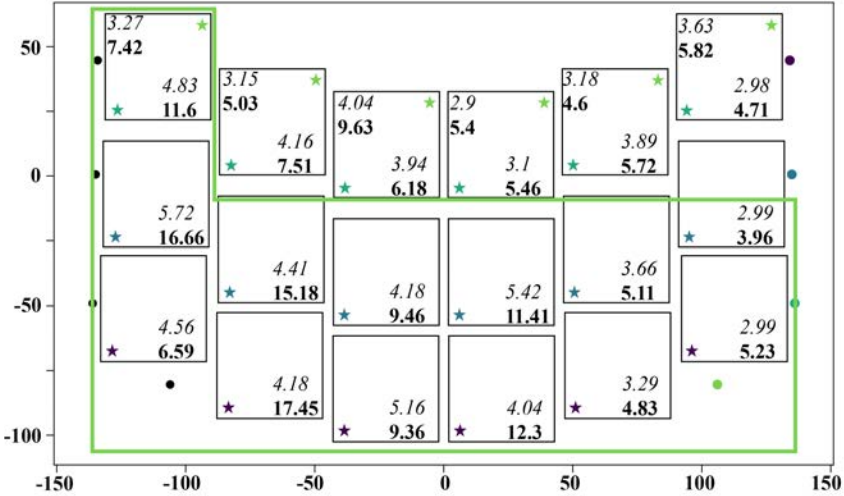

Results

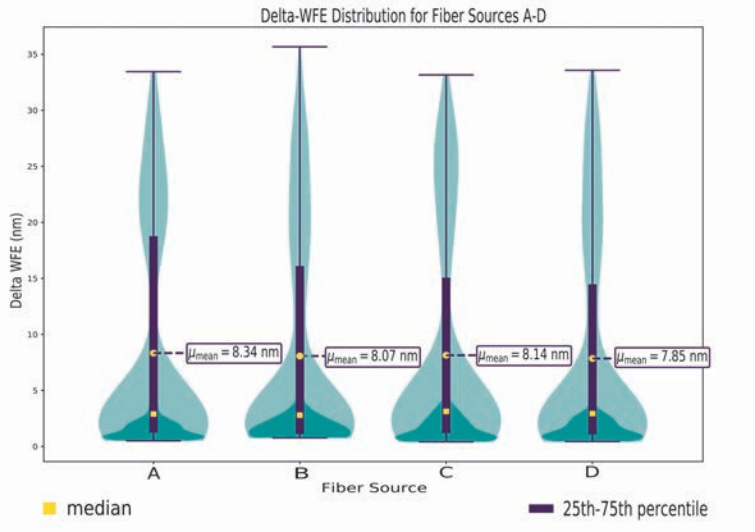

Delta-WFE Distribution for Fiber Sources A-D
Delta WFE (nm)
0
5
10
15
20
25
30
35
$\mu_{mean} = 8.34$ nm
$\mu_{mean} = 8.07$ nm
$\mu_{mean} = 8.14$ nm
$\mu_{mean} = 7.85$ nm
A
B
C
D
Fiber Source
median
25th-75th percentile

Results

Plot of 6 mm and 4 mm radius of decentering for 30 models

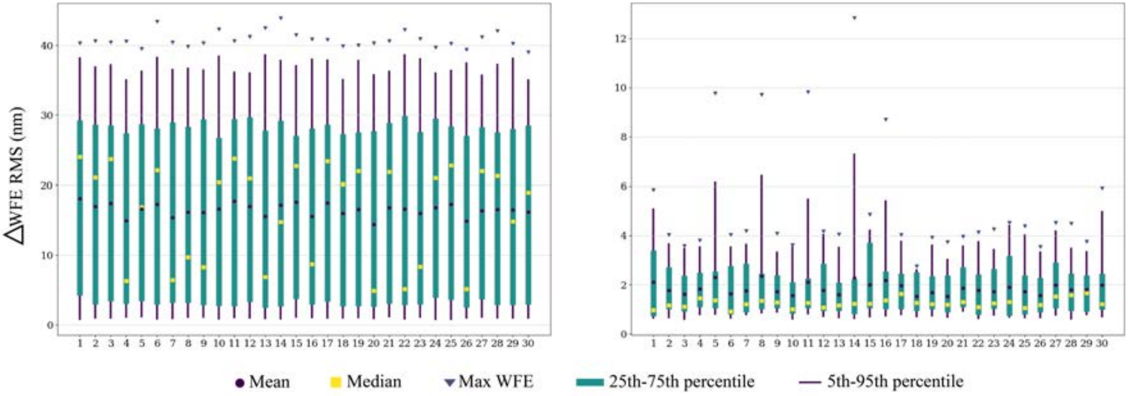

Results

Gravity sag model baseline decentering study

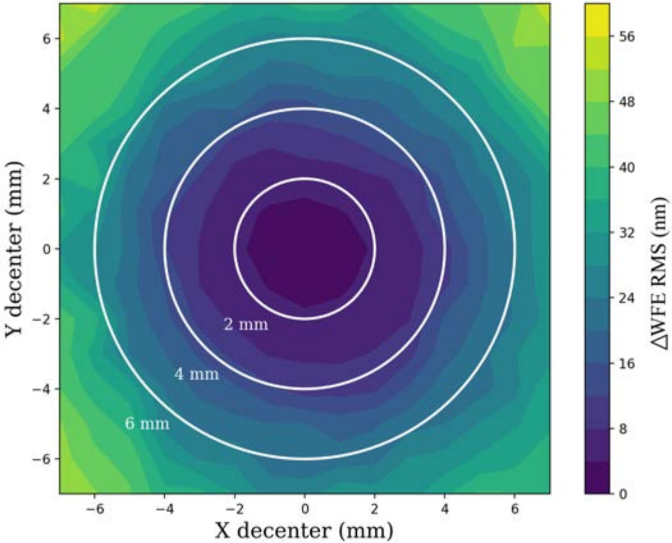

Results

Gravity sag pupil clipping

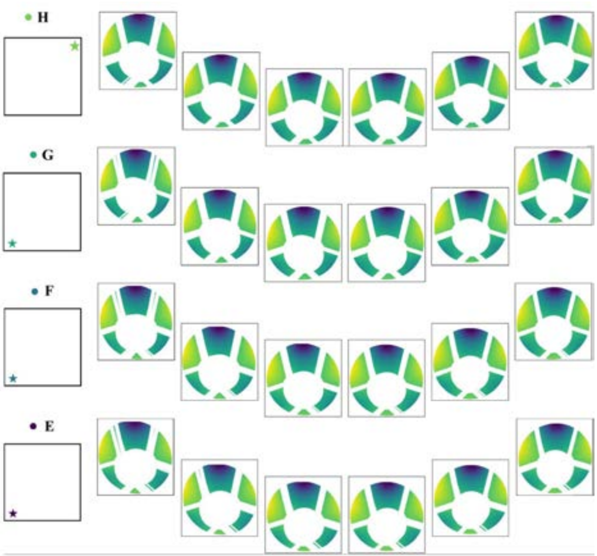

Results
Pupil clipping

Results

Decentering contours across fied of view

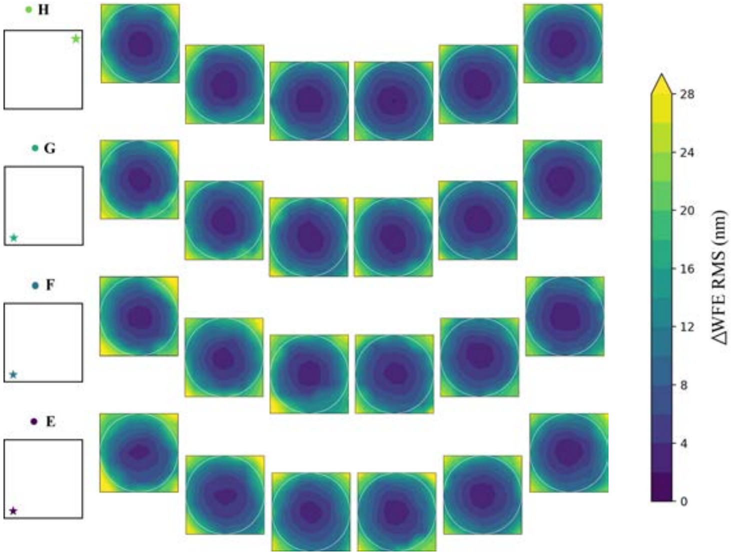

Results

95th percentile and max WFE within 4 mm decentering radius

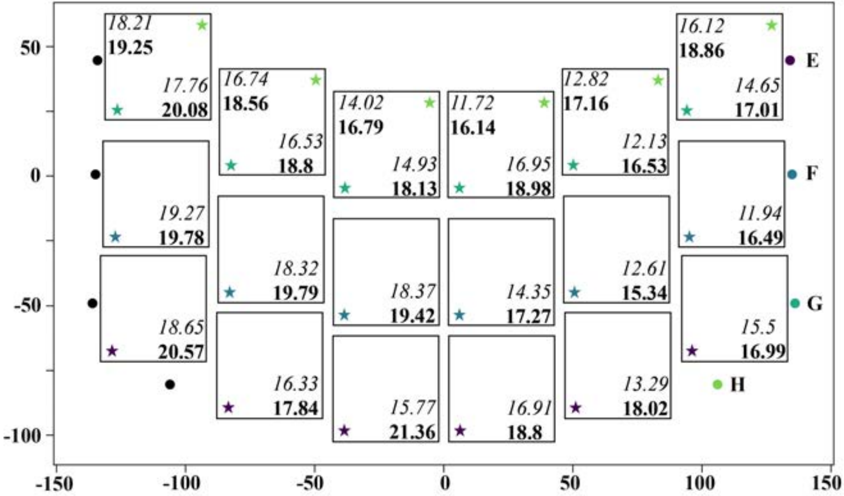

Results
Pupil clipping effects

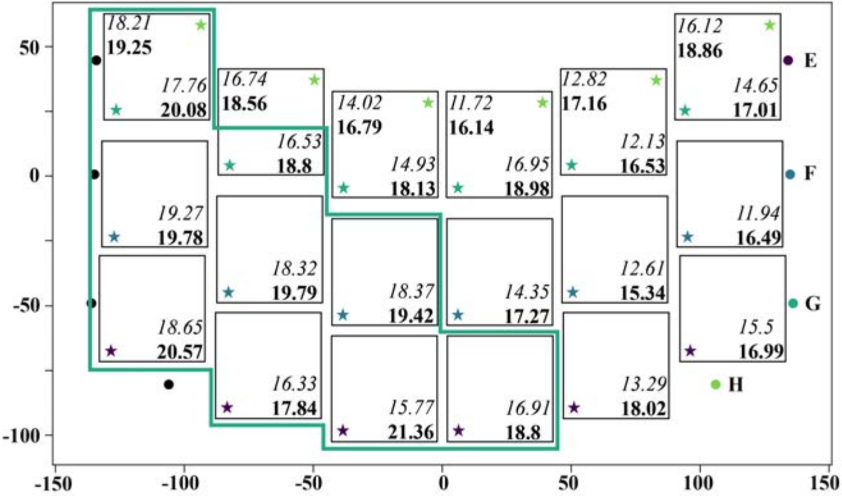

Conclusion

- 4 mm decentering radius fits within error budget for test
- Gravity sag results slightly effected by clipping
- Despite decentering dependent wavefront error and clipping, gravity sag results share similar trends across field of view
- Can confidently use phase retrieval in presence of pupil knowledge error and gravity sag
- Next step is full test simulator

Thank you for listening!

Special thanks to...

- Advisor Prof. Dmitry Savransky
- NASA Goddard & RST WFSC Groups
- My family
- My dog

Questions?

References

- Aronstein, David L. et al. "Wavefront-error performance characterization for the James Webb Space Telescope (JWST) Integrated Science Instrument Module (ISIM) science instruments". In: *Space Telescopes and Instrumentation 2016: Optical, Infrared, and Millimeter Wave*. Ed. by Howard A. MacEwen et al. Vol. 9904. International Society for Optics and Photonics. SPIE, 2016, pp. 63 –80. DOI: 10.1117/12.2233842. URL: https://doi.org/10.1117/12.2233842.
- Bergkoetter, Matthew. "Phase retrieval for chromatic aberrations and wide-field detectors". PhD thesis. University of Rochester. Institute of Optics, 2017.
- Bergkoetter, Matthew D. and Alden S. Jurling. "Data analysis algorithm for double-pass testing of the Roman Space Telescope". In: *Optical System Alignment, Tolerancing, and Verification XIII*. Vol. 11488. International Society for Optics and Photonics. SPIE, 2020, pp. 167 –173. DOI: 10.1117/12.2567347. URL: https://doi.org/10.1117/12.2567347.
- Bolcar, Matthew et al. "Roman Space Telescope Optical System: Overview, Test, and Verification". SPIE Astronomical Telescopes + Instrumentation. 2022.
- Dean, Bruce H. et al. "Phase retrieval algorithm for JWST Flight and Testbed Telescope". In: *Space Telescopes and Instrumentation I: Optical, Infrared, and Millimeter*. Ed. by John C. Mather, Howard A. MacEwen, and Mattheus W. M. de Graauw. Vol. 6265. International Society for Optics and Photonics. SPIE, 2006, p. 626511. DOI: 10.1117/12.673569. URL: https://doi.org/10.1117/12.673569.
- Fienup, J. R. "Phase retrieval algorithms: a comparison". In: *Appl. Opt.* 21.15 (1982), pp. 2758–2769. DOI: 10.1364/AO.21.002758. URL: http://opg.optica.org/ao/abstract.cfm?URI=ao-21-15-2758.
- — ."Phase-retrieval algorithms for a complicated optical system". In: *Appl. Opt.* 32.10 (1993), pp. 1737–1746. DOI: 10.1364/AO.32.001737. URL: http://opg.optica.org/ao/abstract.cfm?URI=ao-32-10-1737.
- Gerchberg, R. W. "A practical algorithm for the determination of phase from image and diffraction plane pictures". In: *Optik* 35 (1972), pp. 237–246.
- Goodman, J.W. *Introduction to Fourier Optics*. Electrical Engineering Series. McGraw-Hill, 1996. ISBN: 9780070242548. URL: https://books.google.com/books?id=QllRAAAAMAAJ.
- Jurling, Alden. "Advances in algorithms for image based wavefront sensing". PhD thesis. University of Rochester. Institute of Optics, 2015.
- Jurling, Alden S., Matthew D. Bergkoetter, and James R. Fienup. "Techniques for arbitrary sampling in two-dimensional Fourier transforms". In: *J. Opt. Soc. Am. A* 35.11 (2018), pp. 1784–1796. DOI: 10.1364/JOSAA.35.001784. URL: http://opg.optica.org/josaa/abstract.cfm?URI=josaa-35-11-1784.
- Jurling, Alden S. and James R. Fienup. "Applications of algorithmic differentiation to phase retrieval algorithms". In: *J. Opt. Soc. Am. A* 31.7 (2014), pp. 1348–1359. DOI: 10.1364/JOSAA.31.001348. URL: http://opg.optica.org/josaa/abstract.cfm?URI=josaa-31-7-1348.
- Smith, Koby Z. et al. "Methodology and Results of James Webb Space Telescope Thermal Vacuum Optical System Alignment Testing and Analysis". In: *34th Space Symposium* (2018).

Phase Retrieval

Nonlinear optimization approach

- Less simple to implement than iterative approach
- Forward model can account for advanced features and is easier to scale with system complexity
- Error metric can be adjusted to account for data artifacts[a][b][c]

[a] Fienup, “Phase-retrieval algorithms for a complicated optical system”.

[b] Jurling, “Advances in algorithms for image based wavefront sensing”.

[c] Bergkoetter, “Phase retrieval for chromatic aberrations and wide-field detectors”.

Phase Retrieval

Algorithmic Differentiation

- Makes nonlinear optimization approach reusable and more robust
- Extends algorithmic differentiation techniques to complex valued problems with multidimensional arrays
- Uses chain rule of partial derivatives
- Works through steps in forward model to propagate gradients
- Use gradients to search along parameters in direction that minimizes error metric[a]

[a] Jurling and Fienup, "Applications of algorithmic differentiation to phase retrieval algorithms".